

BASIC SCIENCE

Responses in Rat Core Auditory Cortex are Preserved during Sleep Spindle Oscillations

Yaniv Sela, MSc¹; Vladyslav V. Vyazovskiy, PhD²; Chiara Cirelli, MD, PhD³; Giulio Tononi, MD, PhD³; Yuval Nir, PhD^{1,4}

¹Sagol School of Neuroscience, Tel Aviv University, Tel Aviv, Israel; ²Department of Physiology, Anatomy and Genetics, University of Oxford, Oxford, United Kingdom;

³Department of Psychiatry, University of Wisconsin-Madison, Madison, WI; ⁴Department of Physiology and Pharmacology, Sackler School of Medicine, Tel Aviv University, Tel Aviv, Israel

Study Objectives: Sleep is defined as a reversible state of reduction in sensory responsiveness and immobility. A long-standing hypothesis suggests that a high arousal threshold during non-rapid eye movement (NREM) sleep is mediated by sleep spindle oscillations, impairing thalamocortical transmission of incoming sensory stimuli. Here we set out to test this idea directly by examining sensory-evoked neuronal spiking activity during natural sleep.

Methods: We compared neuronal ($n = 269$) and multiunit activity (MUA), as well as local field potentials (LFP) in rat core auditory cortex (A1) during NREM sleep, comparing responses to sounds depending on the presence or absence of sleep spindles.

Results: We found that sleep spindles robustly modulated the timing of neuronal discharges in A1. However, responses to sounds were nearly identical for all measured signals including isolated neurons, MUA, and LFPs (all differences $< 10\%$). Furthermore, in 10% of trials, auditory stimulation led to an early termination of the sleep spindle oscillation around 150–250 msec following stimulus onset. Finally, active ON states and inactive OFF periods during slow waves in NREM sleep affected the auditory response in opposite ways, depending on stimulus intensity.

Conclusions: Responses in core auditory cortex are well preserved regardless of sleep spindles recorded in that area, suggesting that thalamocortical sensory relay remains functional during sleep spindles, and that sensory disconnection in sleep is mediated by other mechanisms.

Keywords: auditory cortex, LFP, NREM sleep, rat, single-unit, sleep spindles

Citation: Sela Y, Vyazovskiy VV, Cirelli C, Tononi G, Nir Y. Responses in rat core auditory cortex are preserved during sleep spindle oscillations. *SLEEP* 2016;39(5):1069–1082.

Significance

A long-held hypothesis posits that sleep spindles disrupt relay of sensory signals to the cortex. Here we tested this idea directly for the first time by studying neuronal and LFP responses to sounds in rat primary auditory cortex during natural sleep. We found that when sleep spindles occurred during auditory stimulation, neuronal responses were nearly identical to those observed across NREM sleep. These findings challenge the classic “spindle gating” premise and highlight the need to identify other candidate mechanisms for sensory disconnection during sleep—a topic relevant for understanding hyperarousal and insomnia disorders.

INTRODUCTION

Sleep is defined as a reversible state of behavioral unresponsiveness,¹ and accordingly sleep is characterized by a high “arousal threshold”.^{2,3} Not only do mild external stimuli typically fail to elicit an adequate behavioral response, but they also largely fail to be incorporated in the content of dreams.^{4,5}

The loss of behavioral responsiveness to external stimuli during non-rapid eye movement (NREM) sleep was first ascribed to the thalamus, which switches to a “burst” firing mode that is distinctly different from the tonic mode of operation typical of wakefulness.^{6,7} According to the “thalamic gating” notion, during NREM sleep the thalamus does not effectively relay sensory signals to the neocortex, and attenuated responses to sensory stimulation during sleep have indeed been reported in primary visual cortex,^{8,9} primary somatosensory cortex,¹⁰ and primary auditory cortex.^{11,12} However, recent studies in natural sleep, and in the auditory domain in particular, challenge this view by showing preserved activity in core auditory cortex across wakefulness and sleep.^{13–16}

An influential hypothesis is that sleep spindles, short (0.5–3 sec) oscillations in the sigma (10–16 Hz) frequency band,^{17–21} mediate such thalamic gating.^{22,23} Sleep spindles reflect the intrinsic properties and interactions between inhibitory cells in the reticular thalamic nucleus and bursting thalamocortical relay neurons.²⁴ Given that their generation involves inhibition

of thalamocortical afferents, it was suggested that sleep spindles interrupt the transmission of ascending sensory signals and thus may constitute a mechanism for disconnection during NREM sleep.^{25–28}

The spindle gating hypothesis originated from a study in cats anesthetized with barbiturate,²⁹ in which antidromic cortical stimulation typically led to thalamic discharges but during spindles bursts these evoked discharges were abolished. Along the same line, the amplitude and duration of evoked potentials was reported to be attenuated during the hyperpolarization phase of spindles.³⁰ Since then, a number of studies tried to put the spindle gating hypothesis to the test. Yamadori³¹ delivered sounds during human sleep and reported that (1) auditory stimulation typically evoked K-complexes (high-amplitude isolated slow waves in the electroencephalogram [EEG]³²) but (2) those sounds that coincided with sleep spindles failed to evoke K-complexes, a result that was interpreted as a sign that sleep spindles mediate thalamic sensory gating during sleep. It was also reported that some components of event-related potentials (ERPs) in response to sensory stimulation vary depending on the presence of sleep spindles.³³ More recently, the rate of spindle occurrence during a night of spontaneous sleep was found to be correlated with arousal threshold in a subsequent night of sleep.³⁴ Furthermore, recent simultaneous EEG-functional magnetic resonance imaging (fMRI) studies that delivered tone-pips during human sleep found that auditory cortical

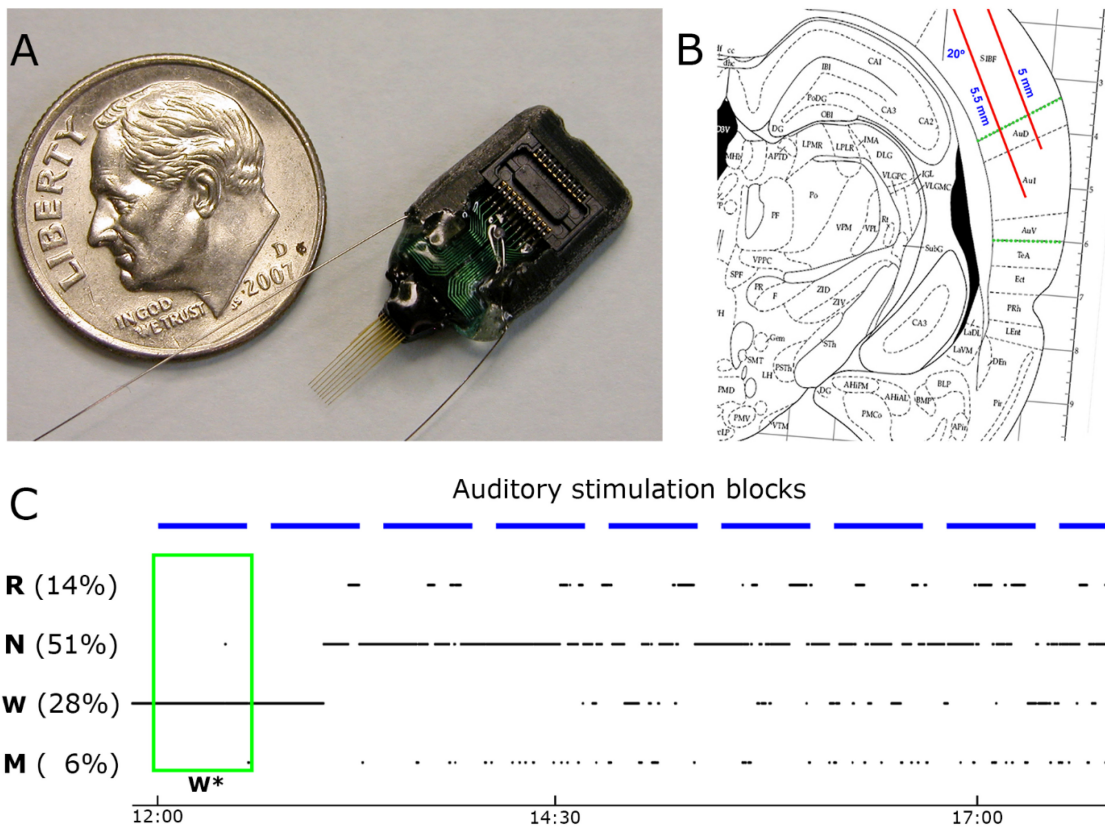


Figure 1—Experimental setup. **(A)** The main implanted recording device was a microwire array consisting of 16-channel (two rows of eight each) tungsten wires of 33 μm and 20–70 k Ω m (Tucker-Davis Technologies, Inc. (TDT), Alachua, FL, USA; spacing between microwires: 175–250 μm ; separation between rows: L–R: 375–500 μm , D–V: 0.5 mm). **(B)** Sketch of surgical plan with oblique implantation of auditory microwires (red lines) superimposed with a coronal diagram of the rat brain 4.5 mm posterior to bregma⁶⁰; dotted green lines denote borders of auditory cortex. **(C)** Example of the auditory stimulation protocol superimposed with changes in vigilance states. Sessions started around 12:00 (time on bottom) and lasted 4–6 h. Experiments included repeated identical blocks of sound stimulation (horizontal blue bars, top), interleaved with 10-min silent intervals. Rats were kept continuously awake during the first block of stimulation (green box, W*) and were left undisturbed during all other blocks. W, N, R, and M correspond to wakefulness, non-rapid eye movement (NREM) sleep, rapid eye movement (REM) sleep, and mixed sleep, respectively. Note that percent time spent in each vigilance state does not add to 100% since epochs containing artifacts were excluded.

responses were different when sounds co-occurred with sleep spindles versus other moments of NREM sleep.^{35,36} Finally, SK2 channel-overexpressing (SK2-OE) mice show enhanced spectral EEG power in the spindle-frequency range and elevated arousal threshold,³⁷ a finding that is often regarded as potential causal evidence for the involvement of sleep spindles in sensory disconnection.

To the best of our knowledge, despite its prevalence, the notion that sleep spindles disrupt relay of sensory signals to the cortex has so far relied on either noninvasive studies in humans, or on electrical microstimulation studies in anesthetized animals, but has yet to be examined directly by studying neuronal responses to sensory stimulation during natural sleep. Here we examined this for the first time by comparing neuronal spiking activity ($n = 269$ units), multiunit activity (MUA), and local field potentials (LFPs) in rat core auditory cortex (A1) of six animals during NREM sleep, comparing responses depending on the presence (or absence) of sleep spindles. Our results show that responses at all levels of examination were nearly identical (differences < 10%), calling into question the long-held role

ascribed to sleep spindles in mediating disconnection during NREM sleep.

METHODS

Data Acquisition

Data acquisition procedures (e.g. surgery, electrophysiology) are described in detail elsewhere.¹⁵ All procedures related to animal handling, recording, and surgery followed the National Institutes of Health Guide for the Care and Use of Laboratory Animals, and were approved by the Institutional Animal Care and Use Committee (IACUC). In brief, three days prior to surgery, adult male Wistar Kyoto rats (Harlan Ltd., $n = 6$) were placed in their home cage within an acoustic chamber for habituation to the experimental environment. Sixteen-channel microwire arrays (Figure 1A) were implanted in the right core auditory cortex (“A1”, Figure 1B), and also in the right motor cortex (three of six animals, Figure S1, supplemental material). In addition, EEG screws were placed over the frontal and parietal

cortices, and neck muscle electrodes were implanted for electromyography (EMG). After surgery, 1 week was allowed for recovery and the experiments started only after the sleep/waking cycle had normalized. All experiments were conducted in a foam-insulated cage placed within a double-wall soundproof chamber. Sounds were played free-field through a magnetic speaker mounted above the animal and contained 24 different sound types (including simple clicks [duration = 1 msec], click-trains [duration = 500 msec], tones [duration = 100/600 msec], as well as complex FM sounds [duration = 100 msec] and AM sounds [duration = 600 msec], and ultrasonic vocalizations [duration = 250–1,000 msec]) in three different volumes (30, 55, and 80 dB SPL), comprising a total of 72 different stimuli. In each 30-min block, each stimulus was presented 15 times (a total of 1,080 trials per block) in a pseudorandom order with inter-stimulus intervals (ISIs, offset to onset) of $1,250 \pm 250$ msec (Figure 1C). We verified that sounds rarely resulted in awakening by careful analysis of the sound-evoked EMG responses. Awakenings were defined by the presence of transient EMG events with amplitude above 3.5 standard deviations occurring within the first 75 msec following sound onset.¹⁵ Upon completion of the experiments, histological verification confirmed that electrodes were located within A1. Data consisted of continuous simultaneous recordings of LFPs and extracellular spike data, together with EEG, EMG, and video. Spikes were detected in the high-pass filtered voltage signal (300–5,000 Hz), and sorted offline using “wave_clus”³⁸ into 137 putative single-units and 132 multiunit clusters (a total of $n = 269$ clusters). Vigilance states were manually scored in 4-sec epochs based on offline simultaneous visual inspection of the EEG, LFP, EMG, and behavior (video) using the SleepSign software (Kissei). Each epoch was categorized as either wakefulness ($15.1 \pm 5.5\%$), NREM sleep ($53.6 \pm 4.3\%$), rapid eye movement (REM) sleep ($19.0 \pm 3.6\%$), mixed epochs ($11.8 \pm 4.7\%$), or artifacts ($1.6 \pm 1.1\%$). Mixed epochs included ambiguous characteristics of more than one sleep stage, for example most such epochs represent gradual transitions between NREM and REM sleep with simultaneous occurrence of frontal slow waves and posterior theta. All subsequent data analysis (e.g., detection of spindles and slow waves, analysis of auditory responses) was carried out offline with Matlab (MathWorks, Natick, MA, USA). Unless stated otherwise, \pm signs represent standard error of the mean (SEM).

Spindle Detection and Verification

We developed an algorithm to automatically detect sleep spindle events in line with previous studies.^{20,39} LFP raw data was resampled to 1,000 Hz, band-pass filtered (using a zero-phase, second order, Infinite Impulse Response Butterworth filter) between 10–16 Hz and the instantaneous amplitude was extracted via the Hilbert transform. Then, two thresholds were set relatively to the mean band-pass signal during NREM sleep: (1) a “detection threshold” (+2 SD above the mean) identified events as potential spindles, and (2) a “noise threshold” (+0.2 SD above the mean) was used to define the start and end of sleep spindle event. To verify specificity for sleep spindles (versus broadband power increases), we excluded any putative

spindle event whose instantaneous amplitude in a control frequency band (20–30 Hz) exceeded a predefined threshold of +4.5 SD above the mean. Finally an event qualified as a spindle if its duration was between 0.5 and 2.5 sec. It should be emphasized that the specific parameters of the spindle detection algorithm (e.g., frequency range, filter settings, thresholds) were optimized after extensive visual inspection to minimize false detections, and a wide range of parameters yielded similar detections and overall results (data not shown). Power spectral density (Figure 2B) was computed on 350-msec time windows centered on spindle peaks or random time-intervals in NREM sleep.

To compute the spindle density across transitions between different vigilance states (as shown in Figure 2C), the rate of spindle occurrence was computed for every four continuous epochs (16 sec) belonging to one vigilance state, and followed by another four continuous epochs that belonged to a different vigilance state. To quantify the statistical significance of specific transitions, we used a one-way analysis of variance (ANOVA) for all 12 transition types, treating each microwire channel in each experiment as an independent measure. To test whether sleep spindles preferentially occurred at a specific phase of slow wave oscillations, we identified those sleep spindles that occurred within $\pm 1,500$ msec from the detected positive LFP peak associated with slow wave OFF periods (see “Slow Wave Detection” section below). Then, the timing of peak sigma-band amplitude in each such spindle event was treated as a singular time-point and binned (as in a spike peristimulus time histogram [PSTH]) relative to the positive LFP peak (OFF period) serving as time zero. The overall results (Figure 2D) represent a histogram averaged across all channels and experiments. Confidence intervals of 99.9% (horizontal green lines) were calculated for each bin by running the same procedure 10,000 times while using random time-points instead of real times of spindles.

Relation between Sleep Spindle Phase and Neuronal Spiking

The coupling of spindle phase and timing of neuronal spikes (Figure 3) was examined as follows: (1) LFP signal was band-pass filtered to the sigma range (10–16 Hz), (2) the instantaneous phase was computed via the Hilbert transform at intervals when spindles occurred, and (3) the phases at which action potentials were recorded at the same microelectrodes were determined. Statistical significance was assessed using the “circular statistics toolbox” for Matlab. Specifically, we tested for nonuniformity in the phase distribution by using the nonparametric Hodges-Ajne test for angular uniformity. Finally, for each neuronal unit that exhibited significant phase-locking to the phase of sleep spindle oscillations, the preferred phase of firing was calculated as the circular mean of all action potential phases.

Global Versus Local Spindles

In those cases where activity was simultaneously recorded in A1 and around the primary motor cortex ($n = 7$ sessions in four animals), we performed spindle detection separately in the LFP signals of the two brain structures. “Global” spindles were defined as those detected spindles across A1 and motor

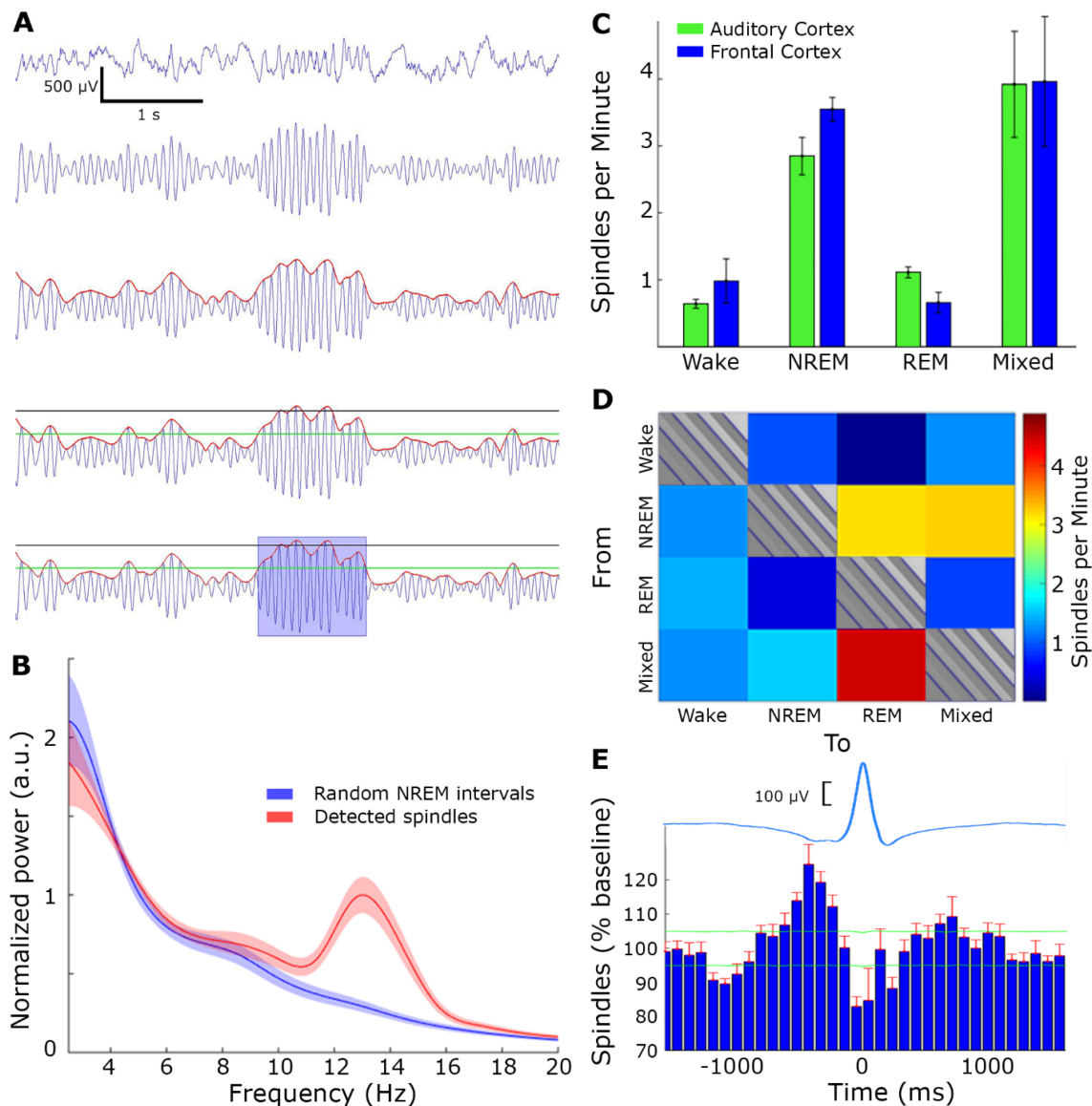


Figure 2—Spindle detection. **(A)** Spindle detection algorithm, from top to bottom: local field potential (LFP) raw data (first row) was band-passed to the sigma band (10–16 Hz, second row) and instantaneous amplitude (red line, third row) was extracted. Detection (black) and noise (green) thresholds were set (fourth row), and duration limits determined the detection of a spindle (blue rectangle, bottom row). **(B)** LFP power spectral density of detected spindle events (red) and random time intervals in non-rapid eye movement (NREM) sleep (blue). **(C)** Number of detected spindles per minute in each state, separately for A1 (green) and motor cortex (blue). Note the higher occurrence during NREM sleep and mixed states. **(D)** Number of detected spindles before state transitions (16 sec) reveal maximal occurrence around transitions between NREM to rapid eye movement (REM) sleep as well as transitions between NREM- > Mixed State- > REM. **(E)** Number of detected spindles around slow waves (time zero corresponds to OFF periods occurring along with LFP positive peak). Top, average LFP slow wave (blue); Bottom, histogram of spindle occurrence (percentage deviation from baseline; mean + standard error of the mean (SEM) across experiments in red). Horizontal green lines, confidence intervals ($\alpha = 0.001$). Note higher spindle occurrence around up states.

cortex that exhibited overlap in their timings, whereas “local spindles” were defined as those events detected only in one brain region without a parallel event in the other region.

Analysis of Auditory Response

After detection of sleep spindles, all auditory trials in NREM and mixed epochs were split to either trials “with spindles” (when the sound onset occurred between spindle start and end times) and trials “without spindles” (all other NREM + mixed trials). We also restricted our analysis only to NREM trials but

this did not affect any results reported (not shown). To statistically compare A1 responses depending on spindle presence, we used the two different approaches: (1) we extracted the P value by using a standard *t*-test, ANOVA, or nonparametric bootstrapping in an attempt to reveal significant differences, (2) additionally, we used bayesian inference to statistically examine the null hypothesis using an online Bayes factor calculator,⁴⁰ defining formally the hypothesis that spindles “should” attenuate the response by 5% to 100% uniformly relative to the control conditions. The outcome of the bayesian statistics, the

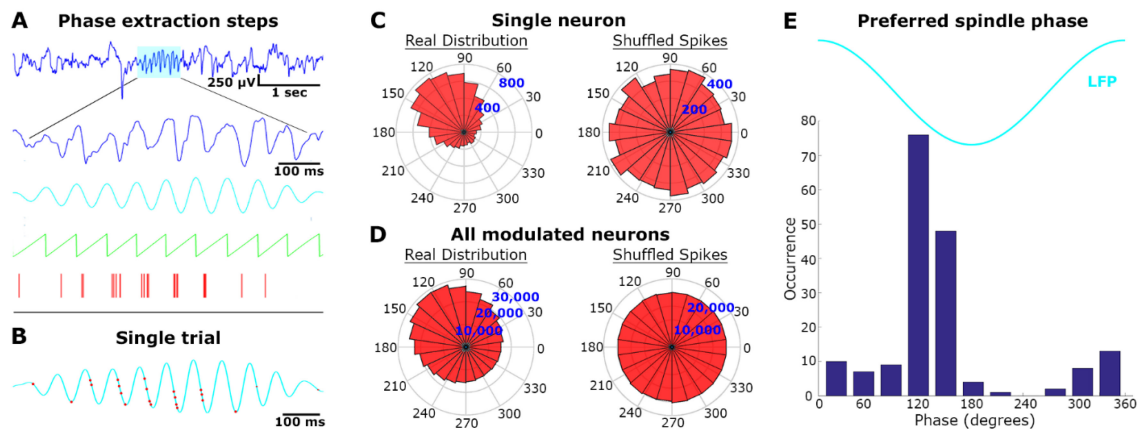


Figure 3—Locking of unit discharges to sleep spindle phase. **(A)** Phase extraction steps: for each detected spindle (first row, cyan), the raw local field potential (LFP, second row) was band-pass filtered (third row, cyan) and the instantaneous phase (green) was compared to precise timing of neuronal action potentials (red bars). **(B)** Single trial example. The band-passed spindle from panel A is shown superimposed with its corresponding neuronal spikes (red dots). **(C)** Single neuron analysis across all spindles: spindle phase angular distribution of spikes from the same unit displayed in A (“real distribution”, left), and distribution of randomly shuffled spikes within each spindle (“shuffled spikes”, right). **(D)** Same as in C for all modulated neurons ($n = 178/269$, 66%). **(E)** Cumulative histogram of preferred spindle phase for all modulated neurons.

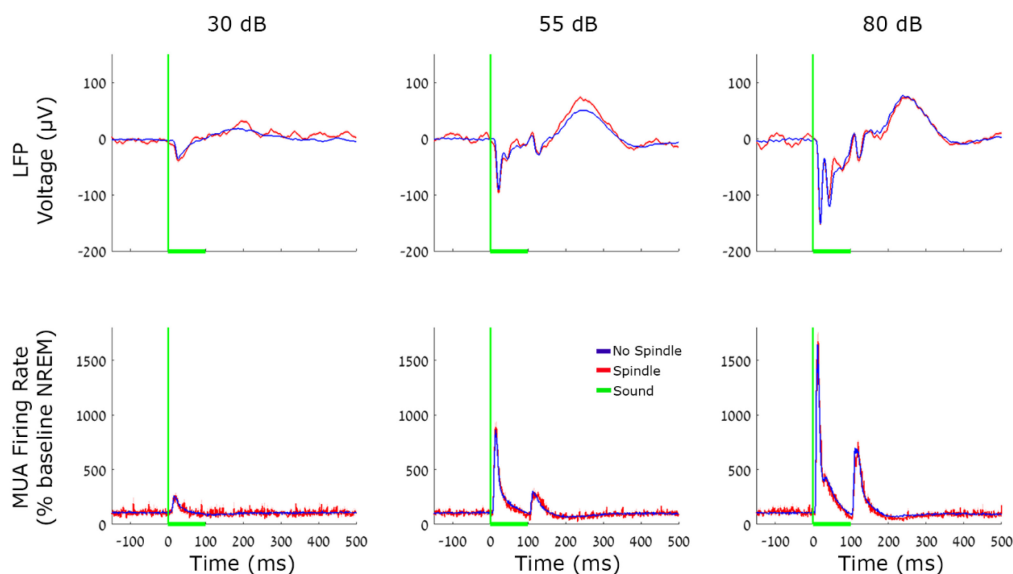


Figure 4—Local field potentials (LFP) and multiunit activity (MUA) auditory responses during spindle and nonspindle trials. Responses of A1 neuronal populations evoked by 100 msec tone pips. Red, spindle trials; Blue, no spindles. Top row, average A1 LFP; Bottom row, average MUA. Columns (left to right) mark sound intensities of 30, 55, and 80 dB SPL. Vertical green lines, sound onset; Horizontal green line, sound duration. Note that both LFP and MUA responses are virtually indistinguishable during spindle and nonspindle trials.

Bayes factor (B), indicates that there is substantial evidence in support of the main hypothesis when $B > 3$, and that there is substantial support for the null hypothesis when its value is below 0.33.

Analysis of LFP and MUA population responses to pure tones (Figure 4) focused on nine pure tone sounds with identical duration (100 msec), each presented at three intensity levels (a total of 27 stimuli). To statistically compare the magnitude of LFP and MUA responses across conditions we first identified the timing of the peak mean response in the 10–30 msec interval after stimulus onset, and then compared

response magnitudes in individual trials via a two-way ANOVA (condition*intensity), and by computing Bayes factor.

Responses of neuronal units to each sound ($n = 72$ sounds) were aligned to sound onset and averaged with 25-msec bins. Onset and offset responses were defined as the first 25-msec bin immediately following either the onset or offset of a sound, whereas sustained responses were defined as those occurring at all other bins, as in our previous study.¹⁵ Changes in firing rates for each response of interest (onset/offset/sustained) were detected by comparing the firing rate to that found during pre-stimulus baseline periods (600 msec), using a Student *t*-test

and corrected for multiple comparisons across time bins with the false discovery rate method [q(FDR) < 0.05].⁴¹ To compare the magnitude of spiking responses in the presence versus absence of sleep spindles we selected for each of the isolated neurons, stimuli and interval type, those cases where a significant response was observed during NREM sleep and at least five trials occurred during sleep spindles. We then calculated the response magnitude separately for trials “with spindles” and “without spindles,” and computed a modulation gain factor using the formula:

$$\%Gain_{a,b} = \frac{a - b}{\max(|a|, |b|)}$$

where *a* and *b* are the mean discharge rate in trials with and without sleep spindles. We further checked whether this gain factor represented a significant deviation from a null (zero-centered) distribution using bootstrapping as follows: We reshuffled the label of all trials (spindle/nonspindle) and calculated the mean gain factor using same procedure, repeating this 10,000 times to estimate the null distribution for gain factors. Finally, the statistical significance (P value) of the difference between spindle and nonspindle conditions was estimated as the location of the real gain factor in relation to the (shuffled) null-distribution. Given our very large data set, weak effects could easily reach statistical significance and therefore, we estimated the effect size above and beyond its significance using Hedge *g*.⁴² A Bayes factor was also evaluated based on the comparison of magnitude of the two conditions with a definition as previously described.

Evaluation of Spindles Terminating upon Auditory Stimulation

To quantify the continuity of sleep spindles after auditory stimulation, we checked the number of spindles lasting at least 500 msec and terminating in different time bins, relative to the onset of 80 dB tone-pips with 100-msec duration. To assess whether the timing of spindle termination for sound trials was significantly different than what may be expected for all spindles, we repeated this analysis for spindles occurring away from auditory trials, and randomly picked a time point along each spindle as a “fictive stimulus onset”. We repeated this procedure 10,000 times to estimate the 95% confidence interval of the null distribution.

Slow Wave Detection

An automatic algorithm was used to detect LFP slow waves (0.5–4 Hz), as described in previous studies.^{43,44} Detected events with wave duration between 0.2 and 1 sec were kept for further analysis (Figure S3A, supplemental material). Artifacts were excluded by removing events with excessive amplitude (more than 4 SD above the mean of the band-pass filtered signal). To minimize false detections and verify that our detected events in the LFP correspond to neuronal ON and OFF periods, we sorted slow waves based on their amplitude and focused on a subset with 40% highest amplitude (different subsets yielded similar results, not shown). Triggering neuronal spiking activity around those events indeed revealed significant modulation of neuronal firing rates as compared with

baseline. For example, in the interval of [–60 40] msec around ON (or OFF) times, neuronal firing rates were significantly modulated (by 15% and 30% on average for ON and OFF periods, respectively; $P < 10^{-50}$ via *t*-test, see also vertical yellow highlight in Figure S3B) and therefore this interval was chosen for future analysis of auditory responses. Firing rate modulations around ON/OFF periods were expressed in % change (normalized relative to the baseline firing rate of each neuronal unit during NREM sleep) to allow pooling results across neurons with variable average firing rates.

Assessment of Slow Wave Phase on Auditory Responses

To compare auditory responses occurring during ON/OFF periods in NREM sleep, we categorized trials to three groups as either (1) occurring during ON periods (if sound onset occurred between –60 to +40 msec around detected LFP negative peak), or (2) occurring during OFF periods (if sound onset occurred between –60 to +40 msec around detected LFP positive peak), or (3) otherwise. Auditory responses were then compared between ON and OFF trials in the same manner described previously for spindle/no-spindle trials, and Bayes factor was computed as the ratio between their likelihoods.

RESULTS

To study the effects of sleep spindles on auditory responses, adult WKY rats were implanted with microwire arrays targeting A1 (*n* = 6) and the motor cortex (*n* = 4) in the right hemisphere (Figure 1). After 1 week of recovery, sleep stabilization, and habituation to stimulation (Methods), acoustic stimuli were presented in nine experimental sessions over a 5-h period during the light phase as animals spontaneously switched between vigilance states. Normal sleep was largely preserved during auditory stimulation experiments, given that trials categorized as wakefulness, NREM sleep, and REM sleep (Methods) exhibited the behavioral and electrophysiological markers associated with these states.¹⁵ Responses to a wide battery of stimuli included tones, clicks and click-trains, complex environmental sounds, rat vocalizations, FM sweeps, and “chirp AM” tones. LFPs, MUA, and isolated neuronal activity (*n* = 269 A1 units in total across all animals) were recorded continuously along with epidural EEG, EMG, and video¹⁵ (see Methods).

Spindle Identification, Characteristics, and Modulation of Neuronal Activity

We detected spindles in the auditory cortex using an automatic algorithm (Methods, Figure 2A, *n* = 102,516 events). Table 1 summarizes the characteristics of detected spindles including density (rate of occurrence per minute), duration, amplitude, and frequency. We verified successful detection via multiple independent measures as follows. First, the power spectral density of detected spindle events confirmed strong sigma power that was not present for random time-intervals in NREM sleep (Figure 2B). Second, spindle occurrence was higher in NREM sleep compared to both REM sleep and wakefulness (Figure 2C, $P < 10^{-9}$, $F = 33.97$ for vigilance state, no effect for region, via two-way ANOVA), and maximal occurrence was observed in transition states, in line with previous reports in rodents.^{39,45,46}

Table 1—Characteristics of sleep spindles in rat auditory cortex.

Rat #	Density (events/min)				Duration (msec)	Amplitude (SD)	Frequency (Hz)
	Wake	NREM	REM	Mixed			
1	0.36 ± 0.03	2.89 ± 0.03	0.64 ± 0.08	—	645.02 ± 2.33	3.60 ± 0.02	13.21 ± 0.03
2	0.31 ± 0.02	2.09 ± 0.06	1.71 ± 0.09	4.72 ± 0.33	642.81 ± 3.49	3.27 ± 0.02	13.56 ± 0.03
3	0.68 ± 0.05	3.19 ± 0.02	1.15 ± 0.03	2.45 ± 0.07	659.52 ± 1.11	3.53 ± 0.05	13.30 ± 0.02
4	0.56 ± 0.04	2.96 ± 0.04	1.52 ± 0.04	4.91 ± 0.22	652.61 ± 1.24	3.40 ± 0.03	13.17 ± 0.02
5	0.74 ± 0.02	2.24 ± 0.03	0.91 ± 0.02	3.81 ± 0.23	660.97 ± 1.93	3.32 ± 0.02	13.15 ± 0.04
6	0.59 ± 0.04	3.22 ± 0.09	1.25 ± 0.05	3.67 ± 0.16	665.91 ± 1.79	3.44 ± 0.05	13.21 ± 0.05
Mean	0.54 ± 0.07	2.76 ± 0.21	1.19 ± 0.17	3.91 ± 0.49	654.47 ± 4.13	3.43 ± 0.05	13.26 ± 0.06

Characteristics of spindles detected in the auditory cortex (mean ± standard error of the mean). NREM, non-rapid eye movement; REM, rapid eye movement.

Table 2—Population responses in spindles/no spindle condition.

		Soft Stimulus	Medium Stimulus	Loud Stimulus
LFP (μV)	No spindle	-36.0 ± 0.5	-91.1 ± 0.6	-151.4 ± 0.8
	Spindle	-39.8 ± 2.8	-96.5 ± 3.0	-152.8 ± 3.6
MUA (% FR)	No spindle	260.0 ± 6.0	861.7 ± 11.9	1,647.0 ± 19.9
	Spindle	264.9 ± 28.6	887.1 ± 55.3	1,671.1 ± 103.9

Mean and standard error of the mean of auditory-evoked response magnitudes measured in the LFP (μV) and in MUA (% FR, firing rate as percent of NREM baseline) during spindle/no spindle conditions. Values correspond to traces in Figure 4. FR, firing rate; LFP, local field potential; MUA, multiunit activity.

Third, focusing more specifically on transition epochs (Methods) revealed high spindle occurrence at transitions from NREM to REM sleep (Figure 2D, $P < 10^{-126}$, $F = 210$, $df = 11$), and maximal occurrence during transitions between NREM sleep and mixed epochs as well as between mixed epochs and REM sleep (reflecting a gradual transition between NREM and REM sleep).^{21,47} Accordingly, spindle occurrence was 2.89 ± 0.18 , 3.73 ± 0.18 , and 4.7 ± 0.2 spindles per minute for NREM-REM, NREM-mixed, and mixed-REM epochs, respectively. Fourth, the distribution of detected events around separately detected slow waves (Methods) exhibited increased occurrence around ON periods as compared to OFF periods (Figure 2E), as expected.^{20,48,49} Taken together, the detected events exhibited the full array of established characteristics of sleep spindles, thereby attesting to successful detection procedures.

Next, we checked whether sleep spindles recorded in A1 modulated the spiking activity of isolated neurons. Although the mean firing rates during spindles did not significantly differ from the baseline during NREM sleep (not shown), the precise timing of action potentials during sleep spindles was robustly modulated by the phase of ongoing sleep spindle oscillations (Figure 3A and 3B). Examining the relation between sleep spindle phase and spike discharges in each neuronal unit separately (Figure 3C, Methods) revealed that the firing of 66% (178/269) of the auditory neurons was significantly modulated by the phase of spindle oscillations (Figure 3D). Most modulated neurons fired maximally around the latter half of the negative slope in the LFP signal (Figure 3E), in agreement with previous studies (see Discussion).

Given that we have recently reported regional occurrence of sleep spindles in humans,^{20,44} we also tested for regional

occurrence of sleep spindles in the rat cortex. As was reported in humans, we found that the majority ($68\% \pm 0.01$) of spindles were local, i.e., only detected in A1 area but not in the motor cortex.

Sleep Spindles Only Show Minimal Effect on Auditory Responses

We compared auditory responses to identical auditory stimuli in trials occurring in NREM and mixed sleep during ($n = 8,342$) and in the absence ($n = 212,329$) of sleep spindles. Population responses (evoked LFP and average MUA, Figure 4) were robustly modulated by stimulus intensity ($P < 10^{-50}$, $F = 1.09 \times 10^3$, $df = 2$ for LFP, and $P < 10^{-50}$, $F = 381.8$, $df = 2$ for MUA via one-way ANOVA), but were indistinguishable between spindle and nonspindle conditions ($P = 0.07$, $F = 3.19$, $df = 1$ for LFP and $P = 0.65$, $F = 0.2$, $df = 1$ for MUA via one-way ANOVA). Examination of multiple *t*-tests for each time interval, even without correcting for multiple comparisons, could also not reveal any significant differences (all $P > 0.09$), and mean differences in response intensity were below 10% (Table 2). In addition, we also used bayesian inference⁴⁰ to formally test whether the changes found here were significantly different than changes in the 5% to 100% range (Methods). We found evidence in favor of the null hypothesis in both the LFP ($B < 0.02$), and the MUA ($B < 0.09$) measurements. We further verified that minimal effects on auditory responses could not be explained by the specific strategy employed to detect spindles: when focusing on a subset of sleep spindles (20%) with the highest amplitude, no significant differences in auditory responses could be revealed (not shown). Finally, we compared the magnitude of auditory responses in each trial to

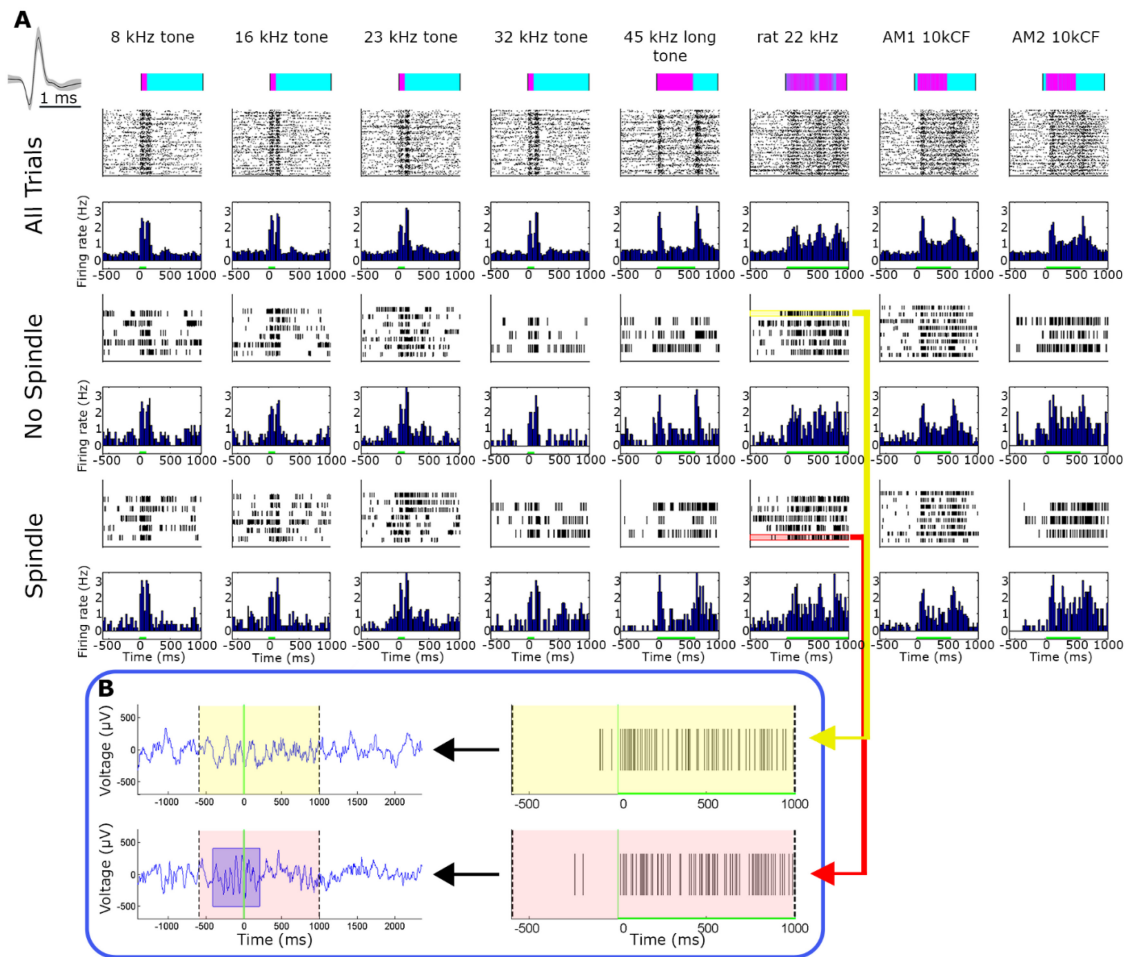


Figure 5—Representative single-unit auditory responses during spindle and nonspindle trials. **(A)** Representative auditory responses of a putative single unit during spindle and nonspindle trials (rows) for eight different stimuli (columns). Rows (top to bottom) correspond to stimuli names and intensities, timing and structure of acoustic stimulus (pink over cyan), followed by raster plots and peristimulus time histograms (PSTHs) for all trials, spindle trials, and non-spindle trials. Inset on upper left shows mean \pm standard error of the mean (SEM) of action potential waveform. Firing rate in all bar graphs is expressed in terms of percent of baseline and is shown with the same scale across all states and stimuli. Note that neuronal responses are nearly indistinguishable visually between spindle and non-spindle trials. **(B)** Two representative trials denoting spike responses during spindle (pink, bottom) and nonspindle (yellow, top) trials. Left panels show A1 local field potential (LFP) whereas right panels show single-unit spiking activity. Note robust response that persists during spindle occurrence.

the sigma power at that time without any detection of specific events (Figure S2, supplemental material) but could not reveal a significant correlation ($|r| < 0.05$).

Next, the spiking responses of isolated neurons were compared between spindle and non-spindle trials. Qualitatively, neural responses to a wide range of sounds were nearly identical (Figure 5). Quantitative analysis across the entire dataset ($n = 269$) performed separately for onset, offset, and sustained responses (Methods) revealed only minor changes in firing rates (all differences $< 6\%$, Figure 6). Only the difference in sustained responses reached statistical significance ($P = 0.04$, Methods) but this likely reflects the large number of trials, because these differences were associated with a minimal effect size (Hedge $g < 0.08$). Moreover, all the estimated Bayes factors substantially supported the null hypothesis ($B < 0.05$, 0.05, 0.11, for onset, offset and sustained responses, respectively). In addition, comparing auditory responses for “local”

versus “global” spindles separately did not reveal significant differences in auditory responses at the level of neuronal populations (LFP, MUA; $P > 0.15$ with two-way ANOVA) nor for neuronal firing rates (mean gain $< 3.5\%$).

During our investigation we noticed that many sounds occurred toward the end of detected spindles, and thus suspected that auditory stimulation may have caused spindles to terminate earlier than usual (Figure 7A). Upon quantitative testing (Methods) we indeed found that the average duration of spindles occurring in conjunction with sounds was significantly shorter than other spindles (mean \pm SEM: 508 ± 0.7 msec versus 660 ± 0.6 msec respectively, $P < 10^{-50}$ via t -test). Upon auditory stimulation with tone-pips, a significant number of spindles (10.5% for 80 dB SPL sounds and 3.5% for 55 dB SPL sounds) terminated shortly (150 – 250 msec) after the sound (Figure 7B) and the number of such spindles (with early termination) was significantly greater than what could be expected

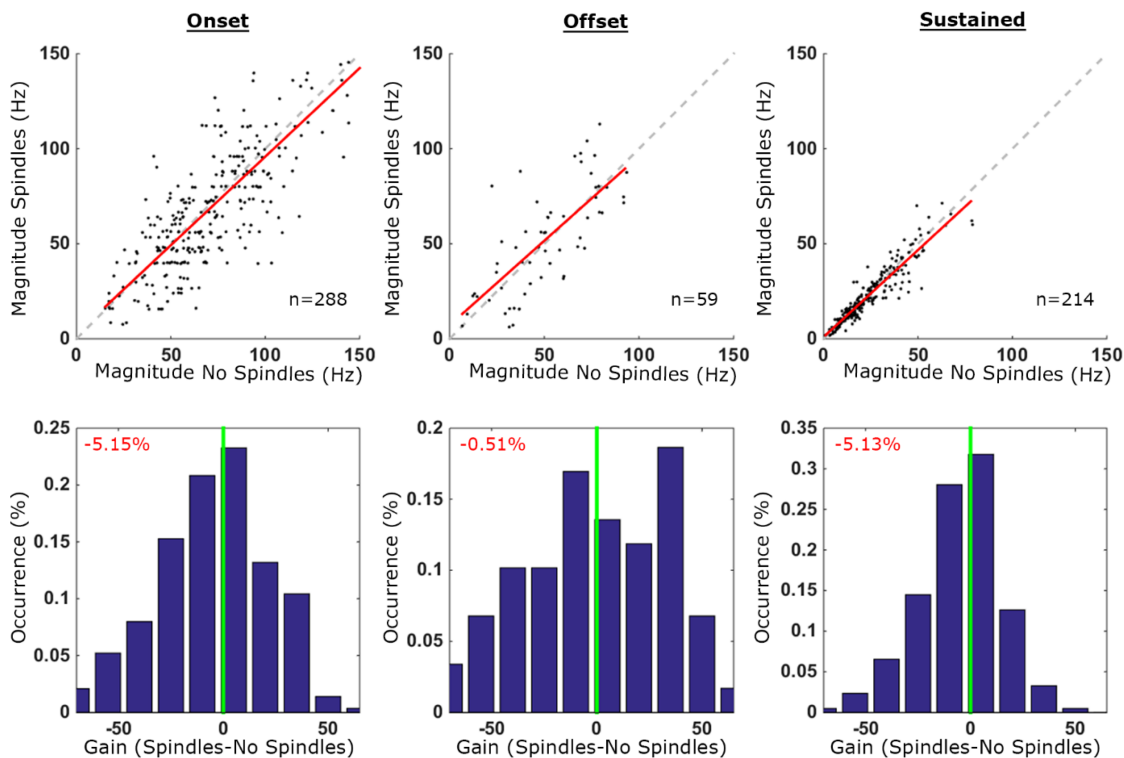


Figure 6—Quantitative comparison of auditory responses in isolated neurons during spindle and nonspindle trials. Quantitative comparison of auditory responses in isolated neurons ($n = 269$) in spindle and nonspindle trials. Columns (left to right) depict results separately for onset, offset, and sustained responses. Top row: scatter plot of response magnitudes (spikes per second, Hz) in spindle trials (y-axis) versus no-spindle trials (x-axis). Each dot denotes the response of one neuronal unit to a specific stimulus ($n = 288, 59$ and 214 conditions for onset, offset, and sustained responses, respectively). Dashed gray line is the identity (45°) line and in red the regression line. Bottom row: distribution of gain factors computed for each stimulus separately. Vertical green line marks zero gain while percentage (red font, top left corners) shows the mean gain factor (none of these mean gain factors were significantly different than zero when evaluated via bootstrapping, see Methods). Positive (versus negative) gain values denote increased response magnitude in spindle trials (versus no-spindle trials). Note that by and large neuronal responses during spindle trials retain response magnitudes.

by chance (Methods). Comparing the time-frequency properties of “interrupted spindles” versus other spindles during loud sounds further demonstrated this effect (Figure 7C) and confirmed that early termination was not accompanied by other noticeable differences (for example, no differences prior to sound onset). Finally, we checked whether auditory-evoked responses may differ between those cases when a spindle was interrupted versus when it was not. Although most LFP and MUA responses did not show any differences, “interrupted spindles” were associated with a significant increase in MUA responses for loud (80 dB SPL) sounds (40.6% increase, $P < 0.012$ uncorrected via t -test).

Effects of Slow Wave Oscillations on Auditory Responses

Given that neuronal population activity alternates between ON (active) and OFF (inactive) periods during NREM slow waves,⁴⁴ silent periods could conceivably constitute an alternative mechanism for sleep disconnection. To examine this possibility, we checked how ON/OFF periods affect auditory responses. We detected individual LFP slow waves ($n = 1,201,275$) and verified that ON and OFF periods were associated with increased and decreased neuronal firing, respectively (Methods, Figure S3). Auditory stimulation trials

were then separated as those occurring tightly ($[-60\ 40]$ msec) around OFF ($n = 16,539$) and ON ($n = 6,389$) periods as identified by LFP peaks (Methods), and compared as was done for spindle and nonspindle conditions. We found that slow wave phase (ON versus OFF) affected the strength of auditory responses in opposite ways (Table 3 and Figure 8), depending on the volume of the sound. During OFF states responses were higher for sounds with high intensity (80 dB SPL), whereas responses during ON states were higher for sounds with low intensity (30 dB SPL). ANOVA confirmed a significant interaction between volume and slow wave phase ($P < 0.0022$, $F = 6.14$, $df = 2$), and *post hoc* (Bonferroni corrected) t -tests further established the statistical significance of these effects ($P = 0.003$, $B = 10^{-4}$, enhanced response for low intensity sounds; $P = 0.94$, $B = 0.87$, comparable response for medium intensity sounds; $P = 0.04$, $B = 55.08$, reduced response for loud sounds). Taken together, the results point to complex effects of slow wave phase on auditory responses, with diverse and opposite influences for different stimulus intensities.

DISCUSSION

In this study, we show that neuronal and LFP responses in A1 of naturally sleeping rats are comparable in the presence

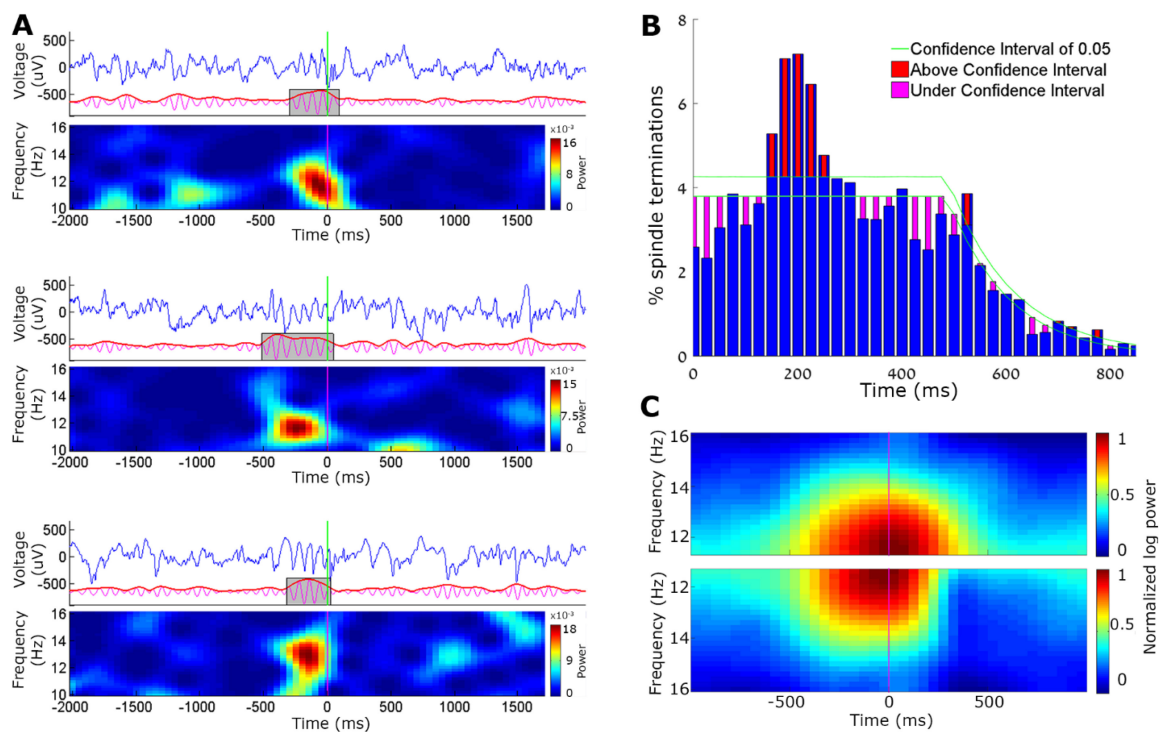


Figure 7—Auditory stimulation leads to early termination of sleep spindles in some trials. **(A)** Three representative example trials for the early termination of spindles upon auditory stimulation. In each example, top row shows the A1 local field potential (LFP, blue), middle row shows the detection procedure (10–16 Hz band-pass filtered signal in magenta, its envelope in red, and detected spindle in gray box), and the bottom depicting time-frequency dynamics (spectrogram). Vertical green line, sound onset. Note the abrupt termination of spindles upon auditory stimulation in all three instances. **(B)** Percentage of spindle terminations after loud tone stimuli. Blue bars show average number of spindle terminations in each time bin, and green lines depict the confidence interval ($\alpha = 0.05$). Red and magenta bars show moments of statistically significant increases and decreases in spindle termination. **(C)** Mean time-frequency (spectrogram) representation of spindle events occurring along with loud tones, separately for (i) all trials (top, symmetric shape), and (ii) for “interrupted spindles” terminating between 150–250 ms after the sound (bottom, asymmetric shape, 30% of trials).

Table 3—Population responses in trials occurring at ON (active) and OFF (silent) periods.

		Soft Stimulus	Medium Stimulus	Loud Stimulus
MUA (% FR)	ON period	312.8 ± 23.4	852.5 ± 36.8	1,505.3 ± 53.2
	OFF period	186.8 ± 31.0	846.9 ± 84.9	1,842.6 ± 186.4

Mean and standard error of the mean of auditory-evoked response magnitudes measured in MUA (% FR, firing rate as percent of non-rapid eye movement [NREM] baseline) during ON/OFF periods. Values correspond to traces in Figure 8A (bottom). FR, firing rate; MUA, multiunit activity.

or absence of sleep spindle oscillations. Comparable results (< 6%) were revealed for different neuronal spiking responses (onset/offset/sustained) and for a wide battery of auditory stimuli (simple tones/clicks versus complex behaviorally relevant stimuli). In addition, we found that auditory stimulation leads to early termination in subset of sleep spindles. Finally, active ON states and inactive OFF periods during NREM slow waves were found to affect the auditory response in opposite ways, depending on stimulus intensity. Despite the influential suggestion that sleep spindles impair thalamocortical sensory transmission,^{22,23,25} the current results suggest that sleep spindles are an insufficient explanation for the mechanisms underlying sensory disconnection in NREM sleep.

Given that the main findings reported here rely on categorizing auditory trials to those occurring in the presence or

absence of sleep spindles, it is important to verify that the detection was truly sensitive and specific. Indeed, detected events showed all the established characteristics of sleep spindles: maximal rates were found in NREM sleep and in transition epochs, whereas occurrence rates in REM sleep and wakefulness were minimal. Furthermore, the high rates during transition epochs specifically reflected transitions between NREM and REM sleep, in line with previous findings.^{21,39,47} Moreover, around slow waves spindles preferentially occurred during active (ON) periods. Importantly, even when focusing our analysis on a subset of the strongest sleep spindles, we could not reveal a trend for response attenuation, nor could we detect significant correlation between response magnitude and sigma power. Altogether, trials categorized as those occurring during sleep spindles can be reliably trusted as such.

We found that sleep spindles robustly modulated the precise timing of neuronal firing in the majority (66%) of recorded neurons. The preferred phase of most modulated neurons, near the trough of intracortically recorded spindles, fits well with previous studies in anesthetized cats and rats^{50,51} as well as naturally sleeping rats.^{52,53} The fact that sleep spindles recorded in A1 robustly affected spiking activity as described in previous studies further strengthens the validity of our detection methods and argues against volume conduction effects.

Auditory responses at different levels of observation (LFP, MUA, isolated neurons) all converged in showing little difference for auditory responses during sleep spindles—suggesting that during natural sleep, spindles do not prevent ascending sensory signals from getting to the cortex. How do the current findings compare with previous results? The original studies examining the effects of sleep spindles on thalamocortical transmission^{29,30} used brief electrical antidromic microstimulation of the ventral lateral motor nucleus of the thalamus in animals anesthetized with barbiturate. A careful review of those pioneering studies reveals that thalamocortical responses during spindles were attenuated in some time intervals, but were in fact even larger in amplitude in other moments during spindle oscillations. These results, although obtained with microstimulation in anesthetized animals, were extrapolated to suggest that spindles mediate disconnection also for external stimuli in natural sleep,²⁵ but this was not examined directly until now. EEG studies in humans reported that the magnitude of the evoked K-complex in response to sounds was attenuated during sleep spindles³¹ but this was challenged by subsequent investigations,⁵⁴ which often showed an augmentation of K-complexes during sleep spindles.³⁶ Along this line, studies that reported changes in ERP components when sounds were delivered in conjunction with sleep spindles³³ were also challenged by later studies. For example, Cote and colleagues reported that sleep spindles only affected high-volume sounds and only when sleep spindles followed stimulus onset.⁵⁵ Last, a recent article⁵⁶ that was published while this work was in review combined scalp and

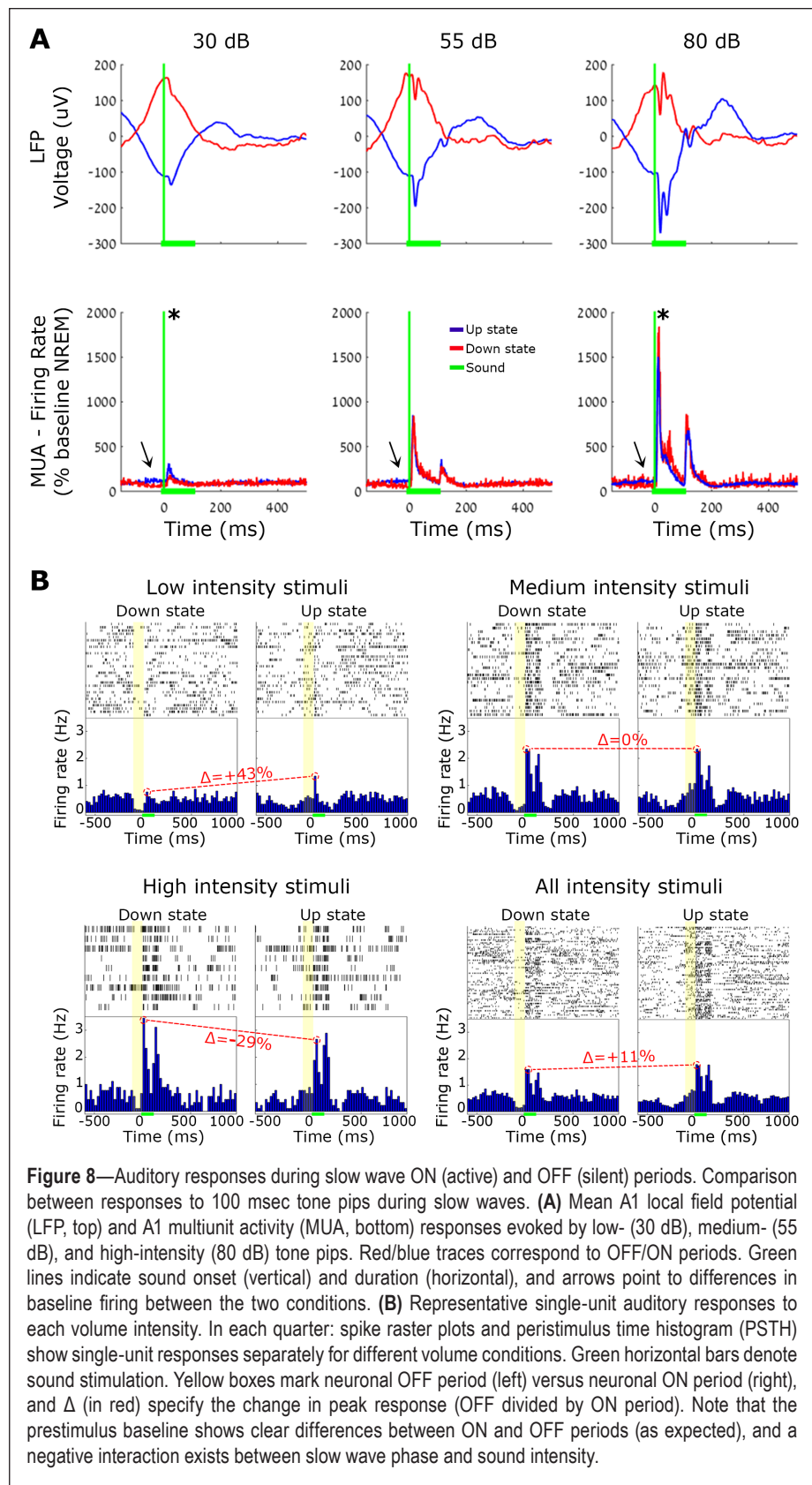


Figure 8—Auditory responses during slow wave ON (active) and OFF (silent) periods. Comparison between responses to 100 msec tone pips during slow waves. **(A)** Mean A1 local field potential (LFP, top) and A1 multiunit activity (MUA, bottom) responses evoked by low- (30 dB), medium- (55 dB), and high-intensity (80 dB) tone pips. Red/blue traces correspond to OFF/ON periods. Green lines indicate sound onset (vertical) and duration (horizontal), and arrows point to differences in baseline firing between the two conditions. **(B)** Representative single-unit auditory responses to each volume intensity. In each quarter: spike raster plots and peristimulus time histogram (PSTH) show single-unit responses separately for different volume conditions. Green horizontal bars denote sound stimulation. Yellow boxes mark neuronal OFF period (left) versus neuronal ON period (right), and Δ (in red) specify the change in peak response (OFF divided by ON period). Note that the prestimulus baseline shows clear differences between ON and OFF periods (as expected), and a negative interaction exists between slow wave phase and sound intensity.

intracerebral EEG in humans to show that spindles had no inhibiting effect on responses to nociceptive stimuli. Together these complementary studies challenge the classical view of inhibitory effects of spindles.

Another important line of research used simultaneous EEG-fMRI to examine regional auditory responses in more detail during sleep spindles.^{35,36} Sleep spindles were detected in scalp EEG while responses in auditory cortex were examined with blood-oxygen-level dependent (BOLD) fMRI, and the authors reported that auditory responses during sleep spindles were more variable. However, several factors may limit the conclusions that can be inferred from these studies. First, auditory responses were characterized with BOLD fMRI as an indirect proxy for neuronal activity, but the extent to which the BOLD signal accurately reflects local neuronal activity during sleep (when neurovascular coupling may change with neuromodulatory changes) remains unclear. Second, higher response variability may reflect a low number of trials occurring during sleep spindles. Third, sleep spindles in scalp EEG may not accurately reflect the local occurrence of spindles in auditory cortex. Indeed, we show here that most sleep spindles in A1 are not simultaneously observed in the motor cortex, extending the notion that most sleep spindles occur locally.^{20,44} Furthermore, other recent studies likewise report that there is only a weak correlation between sleep spindles detected with scalp EEG and those found in the temporal lobe.⁵⁷ Another line of studies show a correlation between spindle occurrence and arousal threshold in both humans³⁴ and SK2-OE mice.³⁷ However, correlative evidence may still reflect a yet undescribed hidden mechanism influencing both the occurrence of sleep spindles as well as sleep stability.

A surprising observation was that a significant number of sleep spindles terminate earlier (~150 msec) than normal upon auditory stimulation, and this was especially true for loud sounds. Our estimated 10% of events terminating abruptly upon sound stimulation is most likely a lower bound, given that the sound-evoked LFP response contains a broadband increase in power (also in the sigma range) that makes it appear that spindles linger more than they actually do. In addition, it is possible that this phenomenon leads to many genuine spindles being missed by the detection algorithm, as it imposes a minimal duration criterion (500 msec) that may not be met when spindles terminate abruptly. An opposite effect, showing that sensory stimuli can also trigger spindles, was demonstrated in previous study.⁵⁸ Thus, future studies are needed to better understand the precise reciprocal interplay between ongoing sleep oscillations and externally evoked activity.

In addition to studying the influence of sleep spindles on auditory responses, we also analyzed in detail how neuronal ON and OFF periods during slow wave oscillations may possibly influence the sound-evoked activity in A1, to examine their possible role as an alternative mechanism underlying sleep disconnection. We found a significant interaction between slow wave phase and sound intensity: OFF periods attenuated the responses to soft sounds, did not affect responses for medium volumes, and increased the response for high intensities. A highly similar pattern was recently reported in a study of intracellular A1 responses in rats.⁵⁹ Given that slow wave phase may result in opposing effects in A1 for sounds of different intensities, it seems unlikely that it can sufficiently explain thalamocortical disconnection generally.

It is also important to note that spindles can only be detected a small percent of the time (< 15%) during natural sleep, and their occurrence is even more rare during REM sleep (Figure 1B); other studies^{20,39} present typical detection rates in other species. Hence, it is difficult to imagine how the occurrence of spindles (or any other transient event) could constitute a satisfactory account of the disconnection that persists throughout sleep. An alternative possibility could be that changes in the neuromodulatory milieu that persist throughout sleep disrupt the propagation of sensory signals via effects at the circuit level.⁵

We wish to explicitly acknowledge the limitations of the current study. First, our auditory recordings were restricted to A1. Although the results establish that auditory thalamocortical transmission to A1 is relatively unimpaired during sleep spindles, it remains possible that sleep spindles impair auditory processing downstream in other auditory (or nonauditory) regions. Second, our study is restricted to the auditory modality. Although the proposed role of sleep spindles in mediating sleep disconnection has been mostly studied with auditory stimuli, it remains possible that other modalities are significantly modulated by sleep spindles, but a recent study reporting preserved sensory responses for nociceptive stimuli in humans argues against such a possibility.⁵⁶

CONCLUSION

Despite the influential and long-standing suggestion that sleep spindles impair thalamocortical sensory transmission, the current results suggest that sleep spindles are an insufficient explanation for the mechanisms underlying sensory disconnection in sleep.

REFERENCES

1. Carskadon MA, Dement WC. Normal human sleep: an overview. In: Kryger MH, Roth T, Dement WC, eds. *Principles and practice of sleep medicine*, 5th ed. St. Louis, MO: Saunders/Elsevier, 2011:16–26.
2. Rechtschaffen A, Hauri P, Zeitlin M. Auditory awakening thresholds in REM and NREM sleep stages. *Percept Mot Skills* 1966;22:927–42.
3. Neckelmann D, Ursin R. Sleep stages and EEG power spectrum in relation to acoustical stimulus arousal threshold in the rat. *Sleep* 1993;16:467–77.
4. Rechtschaffen A. The single-mindedness and isolation of dreams. *Sleep* 1978;1:97–109.
5. Nir Y, Tononi G. Dreaming and the brain: from phenomenology to neurophysiology. *Trends Cogn Sci* 2010;14:88–100.
6. McCormick DA, Bal T. Sensory gating mechanisms of the thalamus. *Curr Opin Neurobiol* 1994;4:550–6.
7. Steriade M, McCarley RW. *Brainstem control of wakefulness and sleep*. Boston, MA: Springer US, 1990.
8. Evarts EV. Photically evoked responses in visual cortex units during sleep and waking. *J Neurophysiol Publ* 1963;26:229–48.
9. Livingstone MS, Hubel DH. Effects of sleep and arousal on the processing of visual information in the cat. *Nature* 1981;291:554–61.
10. Gücer G. The effect of sleep upon the transmission of afferent activity in the somatic afferent system. *Exp Brain Res* 1979;34:287–98.
11. Murata K, Kameda K. The activity of single cortical neurones of unrestrained cats during sleep and wakefulness. *Arch Ital Biol* 1963;101:306–31.
12. Brugge JF, Merzenich MM. Responses of neurons in auditory cortex of the macaque monkey to monaural and binaural stimulation. *J Neurophysiol* 1973;36:1138–58.

13. Peña JL, Pérez-Perera L, Bouvier M, Velluti RA. Sleep and wakefulness modulation of the neuronal firing in the auditory cortex of the guinea pig. *Brain Res* 1999;816:463–70.
14. Edeline JM, Dutrieux G, Manunta Y, Hennevin E. Diversity of receptive field changes in auditory cortex during natural sleep. *Eur J Neurosci* 2001;14:1865–80.
15. Nir Y, Vyazovskiy VV, Cirelli C, Banks MI, Tononi G. Auditory responses and stimulus-specific adaptation in rat auditory cortex are preserved across NREM and REM sleep. *Cereb Cortex* 2013;25:1362–78.
16. Issa EB, Wang X. Sensory responses during sleep in primate primary and secondary auditory cortex. *J Neurosci* 2008;28:14467–80.
17. Loomis AL, Harvey EN, Hobart G. Potential rhythms of the cerebral cortex during sleep. *Science* 1935;81:597–8.
18. Andersen P, Andersson SA. *Physiological basis of the alpha rhythm*. New York, NY: Appleton-Century-Crofts, 1968.
19. De Gennaro L, Ferrara M. Sleep spindles: an overview. *Sleep Med Rev* 2003;7:423–40.
20. Andrillon T, Nir Y, Staba RJ, et al. Sleep spindles in humans: insights from intracranial EEG and unit recordings. *J Neurosci* 2011;31:17821–34.
21. Astori S, Wimmer RD, Lüthi A. Manipulating sleep spindles—expanding views on sleep, memory, and disease. *Trends Neurosci* 2013;36:738–48.
22. Lüthi A. Sleep spindles: where they come from, what they do. *Neuroscientist* 2013;20:243–56.
23. McGinty D, Szymusiak R. Neural control of sleep in mammals. In: Kryger MH, Roth T, Dement WC, eds. *Principles and Practice of Sleep Medicine*, 5th ed. St. Louis, MO: Saunders/Elsevier, 2011:76–91.
24. Steriade M, McCormick D, Sejnowski T. Thalamocortical oscillations in the sleeping and aroused brain. *Science* 1993;262:679–85.
25. Steriade M. *Neuronal substrate of sleep and epilepsy*. Cambridge, UK: Cambridge University Press, 2003.
26. Steriade M. Alertness, quiet sleep, dreaming. In: Peter A, Jones GE, eds. *Normal and altered states of function*. New York, NY: Plenum Press, 1991:279–357.
27. Nunez A, Curro Dossi R, Contreras D, Steriade M. Intracellular evidence for incompatibility between spindle and delta oscillations in thalamocortical neurons of cat. *Neuroscience* 1992;48:75–85.
28. Steriade M. Sleep oscillations and their blockage by activating systems. *J Psychiatry Neurosci* 1994;19:354–8.
29. Steriade M, Apostol V, Oakson G. Control of unitary activities in cerebellothalamic pathway during wakefulness and synchronized sleep. *J Neurophysiol* 1971;34:389–413.
30. Timofeev I, Steriade M. Fast (mainly 30–100 Hz) oscillations in the cat cerebellothalamic pathway and their synchronization with cortical potentials. *J Physiol* 1997;504:153–68.
31. Yamadori A. Role of the spindles in the onset of sleep. *Kobe J Med Sci* 1971;17:97–111.
32. Colrain IM. The K-complex: a 7-decade history. *Sleep* 2005;28:255–73.
33. Elton M, Winter O, Hesenfeld D, Loewy D, Campbell K, Kok A. Event-related potentials to tones in the absence and presence of sleep spindles. *J Sleep Res* 1997;6:78–83.
34. Dang-Vu TT, McKinney SM, Buxton OM, Solet JM, Ellenbogen JM. Spontaneous brain rhythms predict sleep stability in the face of noise. *Curr Biol* 2010;20:R626–7.
35. Dang-Vu TT, Bonjean M, Schabus M, et al. Interplay between spontaneous and induced brain activity during human non-rapid eye movement sleep. *Proc Natl Acad Sci U S A* 2011;108:15438–43.
36. Schabus M, Dang-Vu TT, Heib DPJ, et al. The fate of incoming stimuli during NREM sleep is determined by spindles and the phase of the slow oscillation. *Front Neurol* 2012;3:40.
37. Wimmer RD, Astori S, Bond CT, et al. Sustaining sleep spindles through enhanced SK2-channel activity consolidates sleep and elevates arousal threshold. *J Neurosci* 2012;32:13917–28.
38. Quiroga RQ, Nadasdy Z, Ben-Shaul Y. Unsupervised spike detection and sorting with wavelets and superparamagnetic clustering. *Neural Comput* 2004;16:1661–87.
39. Vyazovskiy VV, Achermann P, Borbély AA, Tobler I. The dynamics of spindles and EEG slow-wave activity in NREM sleep in mice. *Arch Ital Biol* 2004;142:511–23.
40. Dienes Z. Using Bayes to get the most out of non-significant results. *Front Psychol* 2014;5:1–17.
41. Benjamini Y, Yekutieli D. The control of the false discovery rate in multiple testing under dependency. *Ann Stat* 2001;29:1165–88.
42. Hentschke H, Stüttgen MC. Computation of measures of effect size for neuroscience data sets. *Eur J Neurosci* 2011;34:1887–94.
43. Riedner BA, Vyazovskiy VV, Huber R, et al. Sleep homeostasis and cortical synchronization: III. A high-density EEG study of sleep slow waves in humans. *Sleep* 2007;30:1643–57.
44. Nir Y, Staba RJ, Andrillon T, et al. Regional slow waves and spindles in human sleep. *Neuron* 2011;70:153–69.
45. Benington JH, Kodali SK, Heller HC. Scoring transitions to REM sleep in rats based on the EEG phenomena of pre-REM sleep: an improved analysis of sleep structure. *Sleep* 1994;17:28–36.
46. Trachsel L, Tobler I, Borbély AA. Electroencephalogram analysis of non-rapid eye movement sleep in rats. *Am J Physiol* 1988;255:R27–37.
47. Datta S, Hobson J a. The rat as an experimental model for sleep neurophysiology. *Behav Neurosci* 2000;114:1239–44.
48. Steriade M, Nuñez A, Amzica F. Intracellular analysis of relations between the slow (< 1 Hz) neocortical oscillation and other sleep rhythms of the electroencephalogram. *J Neurosci* 1993;13:3266–83.
49. Mölle M, Marshall L, Gais S, Born J. Grouping of spindle activity during slow oscillations in human non-rapid eye movement sleep. *J Neurosci* 2002;22:10941–7.
50. Contreras D, Steriade M. Spindle oscillation in cats: the role of corticothalamic feedback in a thalamically generated rhythm. *J Physiol* 1996;490:159–79.
51. Hartwich K, Pollak T, Klausberger T. Distinct firing patterns of identified basket and dendrite-targeting interneurons in the prefrontal cortex during hippocampal theta and local spindle oscillations. *J Neurosci* 2009;29:9563–74.
52. Peyrache A, Battaglia FP, Destexhe A. Inhibition recruitment in prefrontal cortex during sleep spindles and gating of hippocampal inputs. *Proc Natl Acad Sci* 2011;108:17207–12.
53. Gardner RJ, Hughes SW, Jones MW. Differential spike timing and phase dynamics of reticular thalamic and prefrontal cortical neuronal populations during sleep spindles. *J Neurosci* 2013;33:18469–80.
54. Church MW, Johnson LC, Seales DM. Evoked k-complexes and cardiovascular responses to spindle-synchronous and spindle-asynchronous stimulus clicks during NREM sleep. *Electroencephalogr Clin Neurophysiol* 1978;45:443–53.
55. Cote KA, Epps TM, Campbell KB. The role of the spindle in human information processing of high-intensity stimuli during sleep. *J Sleep Res* 2000;9:19–26.
56. Claude L, Chouchou F, Prados G, et al. Sleep spindles and human cortical nociception: a surface and intracerebral electrophysiological study. *J Physiol* 2015;593:4995–5008.
57. Frauscher B, von Ellenrieder N, Dubeau F, Gotman J. Scalp spindles are associated with widespread intracranial activity with unexpectedly low synchrony. *Neuroimage* 2015;105:1–12.
58. Sato Y, Fukuoka Y, Minamitani H, Honda K. Sensory stimulation triggers spindles during sleep stage 2. *Sleep* 2007;30:511–8.
59. Reig R, Zerlaut Y, Vergara R, Destexhe A, Sanchez-Vives M V. Gain modulation of synaptic inputs by network state in auditory cortex in vivo. *J Neurosci* 2015;35:2689–702.
60. Paxinos G, Watson C. *The rat brain in stereotaxic coordinates*, 4th ed. San Diego, CA: Academic Press, 1988.

ACKNOWLEDGMENTS

The authors thank Noa Bar-Ilan Regev for administrative help and Matthew Banks for help with auditory setup.

SUBMISSION & CORRESPONDENCE INFORMATION

Submitted for publication September, 2015

Submitted in final revised form December, 2015

Accepted for publication December, 2015

Address correspondence to: Yuval Nir, PhD, Sagol School of Neuroscience, Department of Physiology and Pharmacology, Sackler School of Medicine, Tel Aviv University, Tel Aviv 69978, Israel; Tel (lab): 972 3 640 7265; Fax: 972 3 640 7265; Tel (office): 972 3 640 6428; Email: ynir@post.tau.ac.il

DISCLOSURE STATEMENT

This was not an industry supported study. This work was supported by the Human Frontier Science Program Organization long-term fellowship to Dr. Nir, the I-CORE Program of the Planning and Budgeting Committee and the Israel Science Foundation (grant no. 51/11), the Marguerite Stolz Research Fellowship Fund to Dr. Nir, the Sagol School of Neuroscience fellowship to Yaniv Sela., NIMH grant R01MH099231 to Dr. Cirelli and Dr. Tononi, and NINDS grant P01NS083514 to Dr. Cirelli and Dr. Tononi. Dr. Tononi is involved in a research study in humans supported by Philips Respironics. This study is not related to the work presented in the current manuscript. The other authors have indicated no financial conflicts of interest.